Mechanical Properties of Surface-Compressed Wood Resulting from the Compression Ratio and Density Distribution

Zhiqiang Gao,[a b,*] and Rongfeng Huang [b]

Surface-compressed wood, with controllable mechanical properties according to the production process, could be utilized in timber products as a substitute for energy-intensive adhesives, concrete, and metals. The surface compression of wood was carried out in an open hot-pressing system at 180 °C with a compressed thickness of 2 to 18 mm. The surface-compressed wood was treated by atmospheric heat treatment or 0.30 MPa pressurized superheated-steam heat treatment at 180 °C for 2 h. This study investigated the mechanical properties of surface-compressed wood, namely, its bending, compression, and hardness properties. The results showed that the maximum density and average density of the compressed layer surpassed 1.10 g/cm^3 and 0.80 g/cm^3 when the compression ratio was 33%. Moreover, the surface-compressed wood with a sandwich density structure had properties that were comparable to, or even surpassed, raw wood, traditional compressed wood, and some engineered timber products. The specific strength (179 to 203 × 103 m^2/s^2) of surface-compressed wood was slightly higher than other wood-based materials (65 to 197 × 103 m^2/s^2). And the contribution of sandwich structure to MOR and MOE increase was positively correlated with wood surface density. The results obtained from this study could help engineers utilize more fast-growing wood and develop new products and wood connectors. This work may contribute toward the substantial use of surface-compressed wood in the building and construction industries with great benefits to the environment.

DOI: 10.15376/biores.17.3.4280-4296

Keywords: Surface-compressed wood; Sandwich structure; Compression ratio; Mechanical properties

*Contact information: a: College of Agricultural Science, Xichang University, Xichang, 615000, P.R. China; b: College of Materials Science and Technology, Beijing Forestry University, Beijing 100083, P.R. China; *Corresponding author: gzqaandf530@126.com*

INTRODUCTION

The concepts of a green revolution, carbon neutrality, and carbon emissions peak have increased public awareness of the efficient utilization of timber, and the protection of forest lands, particularly virgin forests. As a result, a shift in the available resource base has occurred, from old-growth mature forests to intensively managed, short rotation, forest plantations (Kutnar *et al.* 2008). Many species of trees, such as poplars and Chinese fir in China, are now grown on plantations, where conditions are manipulated to encourage rapid tree growth. Unfortunately, the demand for certain types of wood products cannot be adequately met with this type of wood material, due to their low density (0.3 to 0.5 g/cm^3) and mechanical properties, which prevent them from being used as structural products (Inoue *et al.* 1990; Kutnar *et al.* 2008). However, the poor mechanical properties of low-

density wood can be modified and improved through various combinations of compressive, thermal, and chemical treatments. Wood densification treatment is an eco-friendly wood modification technology based on the combined treatment of wood using elevated temperatures, moisture, and the application of mechanical force (Navi and Pizzi 2015). In addition, this technology can significantly improve the physical and mechanical properties of low-density wood (Laine *et al.* 2016; Zhan *et al.* 2017; Li *et al.* 2018).

Various wood densification methods have been developed (Seborg 1945; Inoue *et al.* 1990; Skyba *et al.* 2008; Navi and Pizzi 2015). The sandwich compression method densifies wood by applying hydrothermal pretreatment to effectively improve the properties of wood with a minimal sacrifice in wood volume, which enables the production of high-density products without destroying the microcellular structure of the wood (Huang *et al.* 2012; Gao *et al.* 2016). Unlike traditional wood compression, compression of sandwich compressed wood can be controlled within a specific area/zone where it is required inside the wood, while another zone in the same wood timber can be left uncompressed or intact. The densities of compressed layer and uncompressed layer are 0.6 to 1.0 g/cm^3 and 0.44 g/cm^3, respectively; the modulus of rupture (MOR) is increased by 20 to 80% (Huang *et al.* 2012; Gao *et al.* 2016). Because the compressed layer(s) and thickness are both adjustable, this technology can minimize wood volume loss caused by compression. Sandwich compressed wood materials suitable for furniture and flooring applications have also been scaled up to the industrial level, and the product can be used as a construction material.

As a type of sandwich compressed wood, surface-compressed wood with a low-density (undensified) core and high-density (densified) faces is analogous to sandwich composite materials. Surface compression has some distinct advantages over bulk compression: the compression process is fast and energy efficient, and the wood volume lost is significantly less (Laine *et al*. 2016; Zhan and Avramidis 2017). Moreover, the thickness and density of the high-density faces can be adjusted according to the practical requirements. Sandwich structures have a high stiffness and strength-to-weight ratio as well as low production costs, and they are quickly becoming the main structural components in many areas of construction (Birman and Kardomatea 2018; Garg *et al.* 2021). They consist of two thin faces with high stiffness and high strength, and a low density and low stiffness core. The faces are typically made of carbon fibers, a glass fiber composite, or metal, while the core is typically made of non-metallic honeycomb, end-grain balsa wood, or closed-cell polymer foams such as polyvinyl chloride or polyurethane (Gdoutos *et al.* 2001). Wood-based sandwich panels can also be found. Plywood-faced sandwich panels with low-density fiberboard can be used as wood-based structural insulated walls and floors have also been developed (Kawasaki *et al.* 2006). In general, the layered materials in a sandwich-structured composite are joined by adhesives, cladding, or anodic bonding. The development of sandwich compressed wood has enabled the development of a novel sandwich material with a low-density core layer and high-density surfaces (Gao *et al.* 2016). The high-density surface can also resist in-plane and bending loads, whereas the low-density core can stabilize the facings and carry shear loads.

This work examined the relevant mechanical properties of surface-compressed wood, namely its bending, compressive, and hardness properties, and demonstrated that it can be used in the production of structural composites. Furthermore, raw poplar timber, other compressed wood, and some engineered timber products were compared.

EXPERIMENTAL

Materials

Twenty-five-year-old Chinese white poplar (*Populus tomentosa*) trees, between 25 to 35 cm in diameter at breast height and an air-dried density of 0.44 g/cm^3, were harvested from a plantation forest in Guan County, Shandong Province in China.. After the timber was dried to 12% moisture content (MC), 400 mm (longitudinal) × 120 mm (tangential) specimens with six different thicknesses of 20, 22, 25, 30, 33, and 38 mm (radial direction) were prepared.

Methods

Surface compression

The surface compression parameters used in this study were chosen based on a previous study (Gao *et al*. 2016; 2019). After the cross- and radial sections of the specimens were sealed with paraffin, the specimens were immersed in water between 0.5 and 5.5 h. The average MC of the specimens was 17% after water immersion.

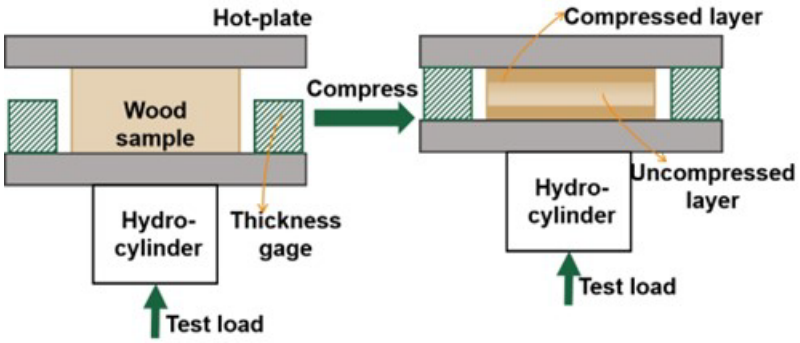

Fig. 1. Diagram showing the thermal compression process

Compression of the specimens was conducted by a hot-press machine (JICA). As shown in Fig. 1, the specimens were placed on the bottom plate of the hot-press machine, and then the top plate quickly made contact with the specimen surface. The temperatures of the top and bottom plates of the hot-press were controlled at 180 °C. Afterward, surface compression in the radial direction was carried out with a pressure of 6.00 MPa. Due to different compressed thicknesses, the total closure time was between 20 to 200 s to achieve a target thickness of 20 mm, while compressed specimens were under pressure for 30 min. Finally, the specimens were removed until the temperature was reduced to 60 °C, with compression ratios of 9%, 20%, 33%, 40%, and 47%. Then the surface-compressed wood was heated with superheated steam for compression fixation, while the compressed wood was treated in a sealed treating vessel with superheated steam at 180 °C for 2 h under a pressure of 0.3 MPa.

Determination of density profiles

Sample sections 50 mm (longitudinal) × 50 mm (tangential) × 20 mm (radial) in size were cut from the centers of the specimens with and without heat treatment. The specimens were then conditioned in a controlled environment of 65% RH and 20 °C for 4 weeks. Their densities were measured using a cross-sectional X-ray densitometer (D-31785, EWS, Hameln, Germany) with a step size of 20 μm, where the sections were scanned from the top to bottom surfaces.

Calculation formulas

The value of the compression set (CR) was calculated by as follows,

$$\mathrm{CR} = \frac{T_1 - T_2}{T_1} \times 100\% \quad (1)$$

where T_1 and T_2 are the dimensions in the compressed direction under ambient conditions before and after densification, respectively.

The average density of the compressed wood increased and the theoretically calculated values of the mechanical properties of the compressed wood were obtained according to the correlation between density and mechanical properties, as shown in Eqs. 2 and 3 (Liu *et al.* 2004),

$$E = \frac{160 \times \rho + 15}{9.8} \quad (2)$$

$$\sigma = \frac{1510 \times \rho - 10}{9.8} \quad (3)$$

where E denotes the modulus of elasticity (MOE) (GPa), σ is the modulus of rupture (MOR) (MPa), and ρ represents the average density of hardwood (g/cm^3).

Morphological structure

All the compressed woods and control specimen were scanned by scanning electric micro-scope (SEM) to investigate the morphological structure change. Specimens were cut from transverse section of compressed layer. The cutting surfaces were sputter-coated gold and scanned in an S4800 SEM (Hitachi, Tokyo, Japan). And the SEM photograph magnification of the surface-compressed wood was 100×.

Testing Standards of the Mechanical Properties

Specimens for mechanical testing were cut from the compressed and control wood samples. And the experiments were performed for both grain directions (R and T) of the compressed material and the control group. The mechanical property test conditions and orientation definitions of the wood grain are shown in Table 1 and Fig. 2. The MOE, MOR, partial compressive strength, total surface compressive strength perpendicular to the grain, compressive strength parallel to the grain, hardness, and surface hardness were measured with a universal mechanical testing machine (Instron 5580, Waltham, MA, USA) according to the standards GB/T 1936.1 (2009), GB/T 1935 (2009), GB/T 1936.2 (2009), GB/T 1939 (2009), GB/T 1941 (2009), and JIS Z2101 (1994), respectively. All specimens were conditioned in a controlled environment with 65% RH at 20 °C for 4 weeks before testing. Samples 20 mm (L) × 20 mm (T) × 20 mm (R) in size were measured from the mechanical specimens after EMC and density testing.

Table 1. Test Conditions and Desired Mechanical Properties

Mechanical properties	Test type	Loading direction	CR (%)
Total surface strength	Compression perpendicular to the grain	R, T	0 9 20 33 40 47
Partial strength		R, T	
MOR	3 p bending	R, T	
MOE	4 p bending	R, T	
Strength	Compression parallel to the grain	L	
Hardness, surface hardness	Hardness	R	

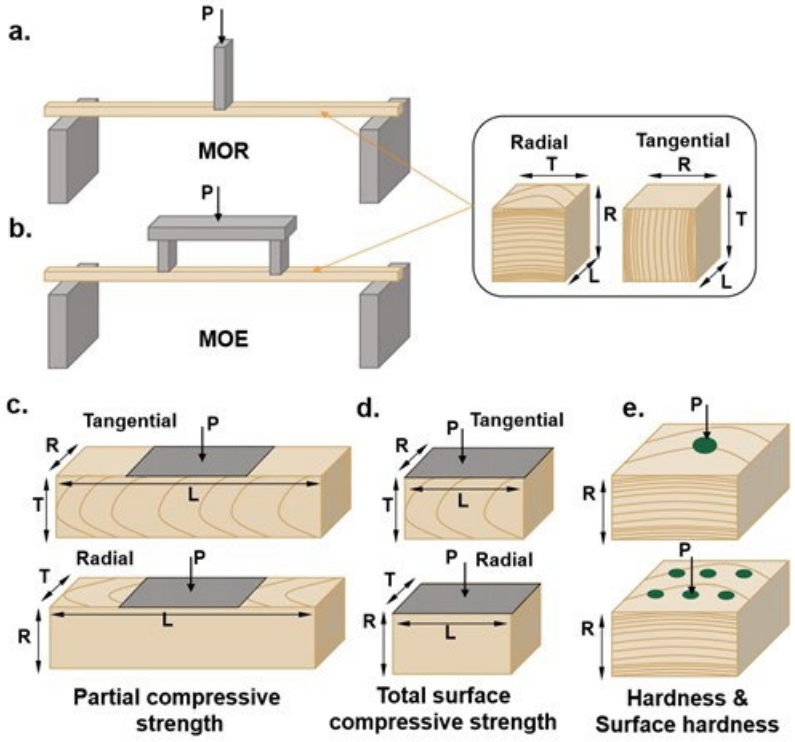

Fig. 2. Schematic diagram of the mechanical property test

RESULTS AND DISCUSSION

Density Distribution Characteristics

As shown in Table 2, surface compression treatment reduced the EMC of the lumber by an average of 1.5%; however, differences between groups with different compression ratios were observed. These results were attributed to the density increase of the surface-compressed wood and reduced hygroscopicity of the surface layers through high-temperature processing (Liu *et al.* 2004). In addition, the lumber density increased proportionally with increases in compression ratio, which was consistent with previous studies (Sandberg *et al.* 2013). Of note, the density and thickness of the top and bottom surface-compressed layers gradually increased as the compression ratio increased;

however, the density of the central layer was almost unchanged until the compression ratio approached 47%, as shown in Fig. 3. Also, the maximum density and average density of the compressed layer surpassed 1.10 g/cm^3 and 0.80 g/cm^3 when the compression ratio was 33%, indicating that the densification phenomenon mainly appeared in the surface layer of the lumber. The surface-compression process used high temperatures and formed steam pressure to obtain conditions above the glass transition temperature in the surface layers of the wood, resulting in high-density surface layers without damage to the cellular structure of the wood.

Table 2. EMC and Density Distribution Characteristics of the Surface Compressed Wood

Compression ratio (%)	EMC (%)	Max density (g/cm^3)	Density [a] (g/cm^3)	Density [b] (g/cm^3)	Density [c] (g/cm^3)
Control	12.20 (0.34)	0.52 (0.02)	0.44 (0.03)	-	-
9%	10.98 (0.43)	0.66 (0.05)	0.63 (0.02)	0.51 (0.03)	0.57 (0.04)
20%	10.74 (0.52)	0.93 (0.09)	0.78 (0.04)	0.75 (0.05)	0.75 (0.04)
33%	10.61 (0.12)	1.12 (0.01)	0.83 (0.02)	0.97 (0.04)	0.83 (0.07)
40%	10.63 (0.28)	1.13 (0.05)	0.86 (0.03)	0.97(0.05)	0.99 (0.06)
47%	10.55 (0.02)	1.16 (0.02)	0.87 (0.02)	0.98 (0.02)	1.00 (0.06)

Note: a represents the average density of the compressed layer, b represents the average surface density of 0.32 mm, and c represents the average surface density of 2.82 mm. And the numbers in parentheses represent the standard deviation.

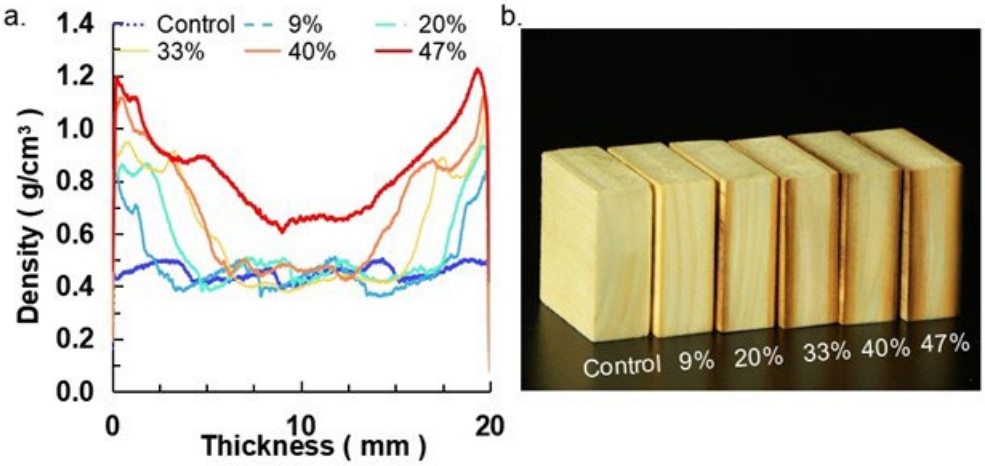

Fig. 3. Density distribution (a) and photograph (b) of the surface-compressed wood

Cellular Deformation

Figure 4 shows cross-sectional SEM images of the control and compressed wood samples. *Populus tomentosa* is a diffuse-porous wood; thus, the vessels were arranged in single or diametrically multiple tube holes. The numerous pits in the vessels were conducive to hydrothermal diffusion, and the porosity was about 70% (Yan 2010; Liu *et al.* 2004), providing a good structural foundation for compression processing. With an increase in the compression ratio, the surface cells gradually began to undergo buckling deformation, the cell cavities showed decreased flexibility, and the void ratio decreased.

The vessel cells and the surrounding parenchyma cells deformed first, followed by the wood fiber cells. When the compression ratio increased to 40%, the surface vessel cells changed from oval to narrow and flat in shape, and the wood fiber cells started to undergo buckling deformation. However, most of the voids were still visible. At a compression ratio of 47%, the cells adjacent to the surface were very dense and had very low porosity.

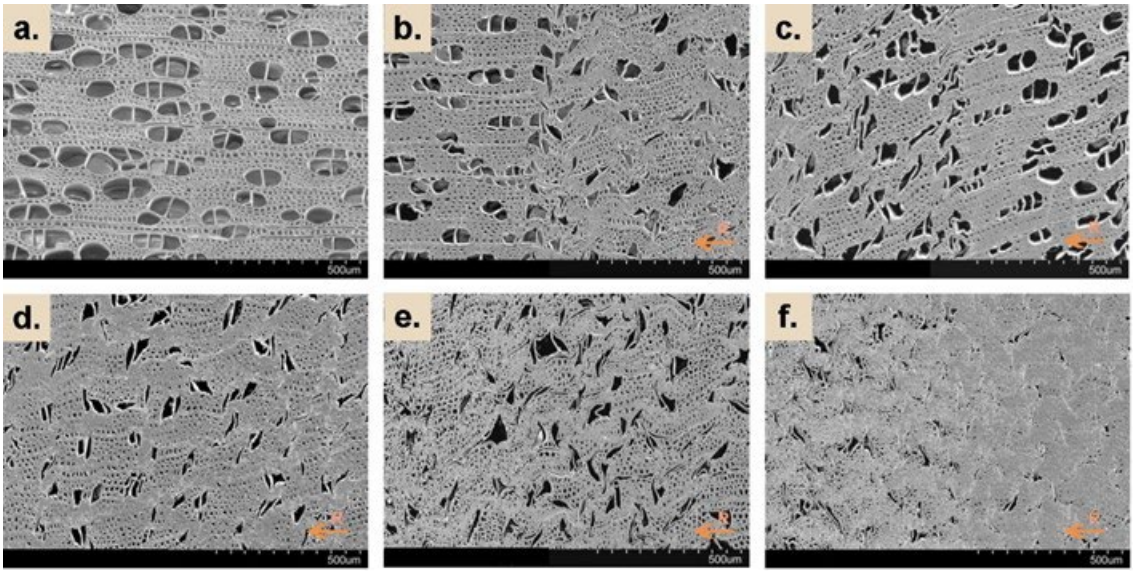

Fig. 4. SEM photograph of the surface-compressed wood for each compression ratio condition. (a. control; b. CR=9%; c. CR=20%; d. CR=33%; e. CR=40%; f. CR=47%. The arrow direction indicates the compression direction.)

Bending Properties of Surface-Compressed Wood

The elastic modulus and bending strength of wood indicate its ability to resist bending deformation and to bear transverse loads within the proportional limit, respectively (Liu *et al.* 2004). Figure 5 a and b shows the change curves of the tangential and radial MOE and MOR of the surface-compressed wood with an increase in the compression ratio. The tangential and radial MOE increased gradually as the compression ratio increased, and the values increased to 20.7 and 23.9 MPa, respectively, when the compression ratio was 47%. In addition, the change trend of the MOR was consistent with MOE. To further clarify the proportional relationship between the changes in mechanical properties relative to the density after compression treatment, the mechanical and density values of the compression group were standardized based on the reference. As shown in Fig. 5c and d, the line for slope 1 was the ideal line that corresponded precisely with the density increase and characteristic value increase rates. The normalized distribution of the bending properties was almost identical to the ideal straight line. However, the difference between the bending properties in the tangential and radial directions was significant, and it initially increased and then decreased with an increase in the compression ratio. When the compression ratio increased to 40%, the differences in MOE and MOR increased to the maximum values, and were 4.11 GPa and 23.4 MPa, respectively. The differences in tangential and radial bending properties were mainly due to the structure density distributions and cell arrangements of the surface-compressed wood. As shown in Fig. 6, the radial density distribution of the surface-compressed wood followed a sandwich structure model with a high surface density and low central density. Of note, the stress distribution of the surface-

compressed wood also gradually decreased along the surface to the center during bending property measurements. This was exactly consistent with the density distribution of the surface-compressed wood (Gao *et al.* 2016). However, the density distribution of the surface-compressed wood was even in the tangential direction, and the surface density under maximum stress was significantly lower than in the radial direction. Therefore, the surface-compressed wood showed better bending resistance under radial loading.

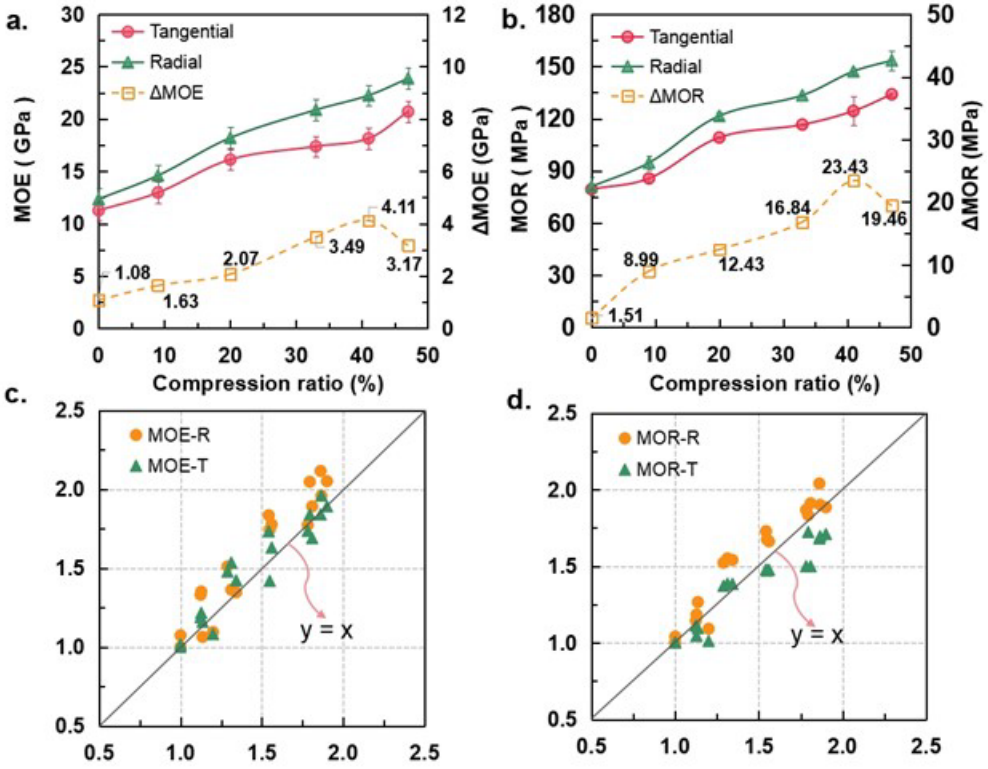

Fig. 5. Effects of compression ratio on the flexural resistance (a, b), relationship of compressed wood under bending *vs*. density (c, d)

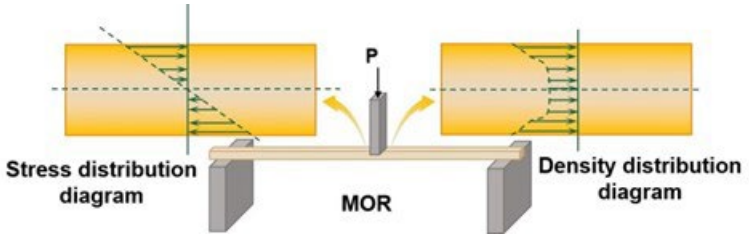

Fig. 6. Schematic diagram of the stress and density distributions in the load direction during the MOR test

In addition, compared with the traditional integral compressed wood, the surface-compressed wood showed better mechanical properties due to the high specific strength and high specific rigidity resulting from the density advantages of the sandwich structure. When the compression extent was 33%, the MOE and MOR of the surface-compressed wood increased by 52.6% and 36.4%, respectively, compared with the control. Notably, the integral compression method also effectively improved the mechanical properties of the wood (Navi *et al.* 2015). Kitamori *et al*. (2010) found that the MOE and MOR of

integral compressed wood increased by nearly 35% and about 30%, respectively, when the compression was 33%. However, the MOE and MOR of the surface-compressed wood were significantly improved by 69.1% and 64.9% at the same compression ratio. As mentioned above, the surface-compressed wood formed a gradient distribution structure with a high surface density and low central density, while the surface layers of the materials had maximum tensile or compressive stresses in the bending performance test. Moreover, the closer the position to the neutral layer, the smaller the stress (Anshari *et al.* 2012; Wang *et al.* 2018).

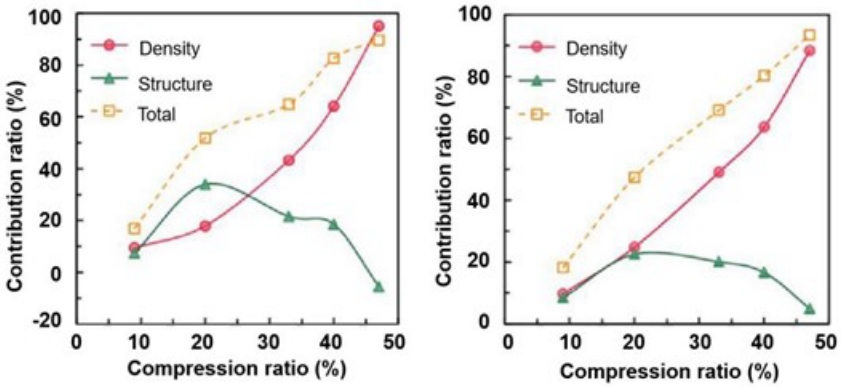

Fig. 7. The contribution of density and structure toward increases in MOE (a) and MOR (b)

Figure 7 shows the contributions of density and structural characteristics toward the bending performance improvements of the surface-compressed wood, given the advantages of the radial density structures of the surface-compressed wood. As described in the materials and methods section, the theoretical values of the wood MOE and MOR were calculated after the density increased, and the actual values were obtained through mechanical property measurements. The theoretical and actual increases of MOE and MOR were obtained by comparing the calculated and actual values with the values of the control wood. The theoretical increase was the contribution of density, and the difference between the actual increase and theoretical increase was the structural contribution caused by the sandwich structural characteristics. With an increase in the compression ratio, the density of the compressed wood increased and the contribution of density toward MOE and MOR also gradually increased. The contribution of the sandwich structure first increased and then decreased, which was closely related to the maximum density of the surface layer subjected to the maximum stress in the radial direction of the compressed wood. As shown in Table 2, the density of the surface layer gradually increased from an initial density of 0.44 g/cm^3 to over 1.10 g/cm^3, and the maximum density of the surface layer increased slowly; thus, the contribution of the sandwich structure decreased. This was the sandwich density structure of the surface-compressed wood was such that sandwich compression technology could improve the bending resistance of the wood while minimizing its volume.

Compressive Properties of Surface Compressed Wood

Figure 8 shows a bar diagram of the transverse compressive strength of the compressed wood as a function of compression ratio. With an increase in the compression ratio, the transverse grain compressive strength of the wood gradually increased, and the partial-surface transverse compressive strength was always higher in the radial direction

than in the tangential direction. This was initially supported by the radial wood rays (Liu *et al.* 2004; Li 2014). Then longitudinal arrangement of the high-density fiber bundles on the surface layers in the radial direction carried larger loads during the partial-surface compressive strength test (Bao *et al.* 2016; Gao *et al.* 2016). The variation trend for the full-surface compressive strength differed from partial-surface compressive strength. For the control wood, the radial full-surface compressive strength was higher than the tangential direction, which was also due to the effects of the wood rays (Cao *et al*. 2016). When the compression ratio increased to 33%, the full-surface compressive strength in the tangential direction was greater than in the radial direction, and the low-density layer in the center was initially subjected to the loads during the radial full-surface loading process (van der Put 2008; Marat-Mendes *et al.* 2020). Thus, the high-density compression layer only played a supporting role in the chordal full-surface test, and the full-surface compressive strength in the tangential direction was higher than in the radial direction. According to the actual usage environment and requirements of the material, the force direction of the material could be reasonably arranged.

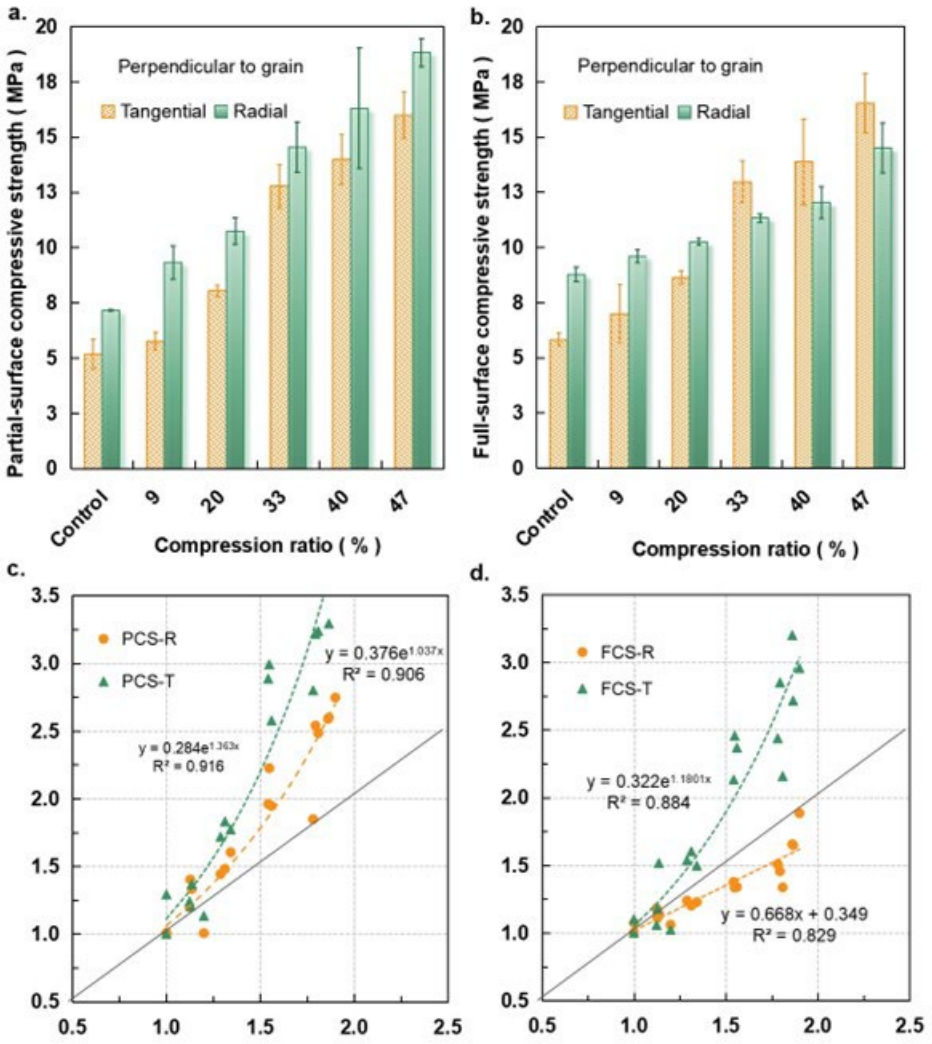

Fig. 8. Partial-surface and full-surface compressive strength (a, b) perpendicular to the grain of the compressed wood and relationship of the compressed wood in compression *vs*. density (c, d)

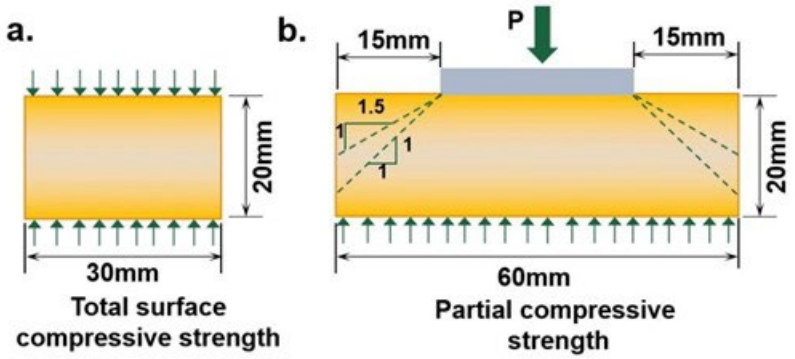

Fig. 9. Stress distribution during compressive strength testing perpendicular to the grain of the compressed wood, (a) total surface compression, and (b) partial compression

In addition, the partial-surface compressive strength of the surface-compressed wood was higher than the full-surface compressive strength, which was mainly related to the stress distribution during the compression process. Under the action of intermediate partial load, the wood was transformed from the elastic to the plastic stage. In the plastic deformation stage, a stress redistribution effect occurred in the compressed wood following the slip-line theory (van der Put 2008; Leijten *et al*. 2010, 2016; Cao, *et al*. 2016). As shown in Fig. 9, when the strain was small, the stress diffused along an oblique line with a slope ratio of 1:1 (45°). When the strain was large, the stress diffused along an oblique line with a slope ratio of 1:1.5 (34) (van der Put 2008; Leijten *et al.* 2010, 2016). Therefore, during the partial-surface compression test process, the two ends that were not directly under pressure carried a portion of the stress component and the partial-surface compressive strength was higher than the full-surface compressive strength. In addition, horizontal splitting of the specimens under the partial-surface compression strength testing was consistent with the internal stress diffusion path (Cao *et al*. 2016), while the specimens under full-surface compression strength testing were mainly separated, with slip between the wood fibers along the grain direction (Zhong *et al.* 2015; 2016).

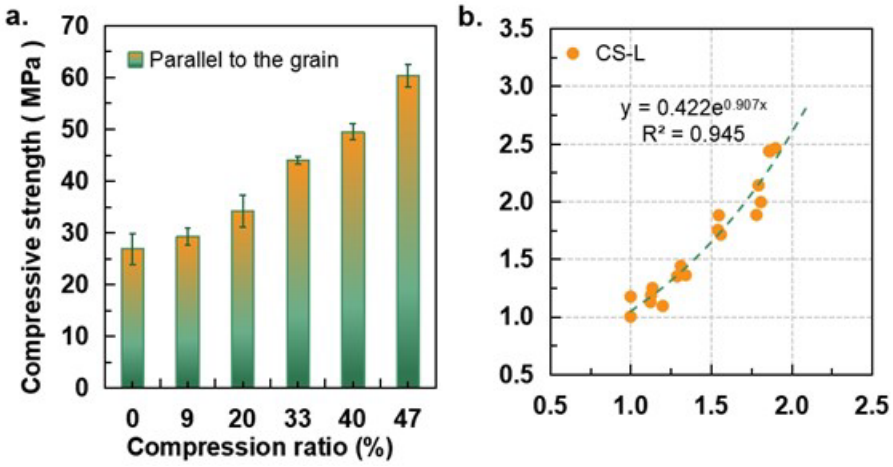

Fig. 10. Compressive strength parallel to the grain of the surface-compressed wood (a) and relationship of the compressed wood in compression *vs*. density (b)

Figure 10 shows the axial compression strength of the surface-compressed wood. With an increase in the compression ratio, the axial compression strength gradually increased, and the maximum value was 60.4 MPa, which was 124% higher than the control. The increase in compressive strength along the grain was mainly due to the substantial amount of wood bearing force per unit area, where the fibrous tissue arranged along the grain increased. The proportional relationship between the change in axial compression strength relative to density is shown in Fig. 10b, indicating that the line for slope 1 was the ideal line that precisely corresponded to the density increase and characteristic value increase rates. The high-density surface layer and the low-density central layer formed a parallel structure in the longitudinal direction, and the fiber tissue of the high-density surface layer could take on greater compression loads, as the surface layer density was higher and the fiber organization was denser.

Hardness and Surface-Hardness of Surface-Compressed Wood

Hardness is a solid property that indicates rigidity and resistance to surface pressure; thus, surface hardness indicates the ability of a solid surface to resist deformation or damage. A material with good hardness or surface hardness can effectively prevent surface damage and prolong its service life. In this work, the difference between hardness and surface hardness was mainly in the depth of the steel ball that was pressed into the wood during the testing process. Therefore, the density distribution of the compressed wood, especially the average densities at 2.82 and 0.32 mm below the surface, were a key influence on the wood and surface hardness. As shown in Fig. 11a, b, and c, the average densities at 2.82 and 0.32 mm below the surface both increased to 1.0 g/cm^3 initially and then remained almost unchanged, and the change points for the compression ratio were 40% and 33% respectively. The surface hardness was in step with the average density of 0.32 mm below the surface. It increased from 6.92 to 19.06 MPa as the thickness and density increased, when the compression ratio increased to 47%. However, the hardness was not only affected by the average density at 2.82 mm below the surface, but also by the thickness of the compressed layer. The average density at 2.82 mm below the surface increased to about 1.0 g/cm^3 initially and then showed few changes; however, the hardness gradually increased with increasing compression ratio, which was attributed to the thickness of the compressed layer.

The proportional relationship between the change in hardness and surface hardness relative to the density is shown in Fig. 11d, where the line for slope 1 was the ideal line that precisely corresponded to the density of the compressed layer increase and the characteristic value increase rates. When the compression was 20%, the hardness and surface hardness increased by 54.56% and 62.97%, compared to the control, similar to the research results obtained by Cai *et al.* (2013). The hardness and surface hardness of the compressed wood still increased by 122.03% and 129.61% compared to the control wood. Morsing (2000) found that when the compression amounts of the whole compressed wood were 20% and 33%, the hardness of the wood only increased by about 40% and 85% compared to the control wood (Kutnar *et al.* 2009). The density of the surface core layer increased uniformly during the overall compression process of the wood (Morsing 2000), while compression of the wood surface created a layered material with a high-density surface layer and a low-density core layer. Therefore, the high-density surface layer could resist greater ball pressure during hardness testing.

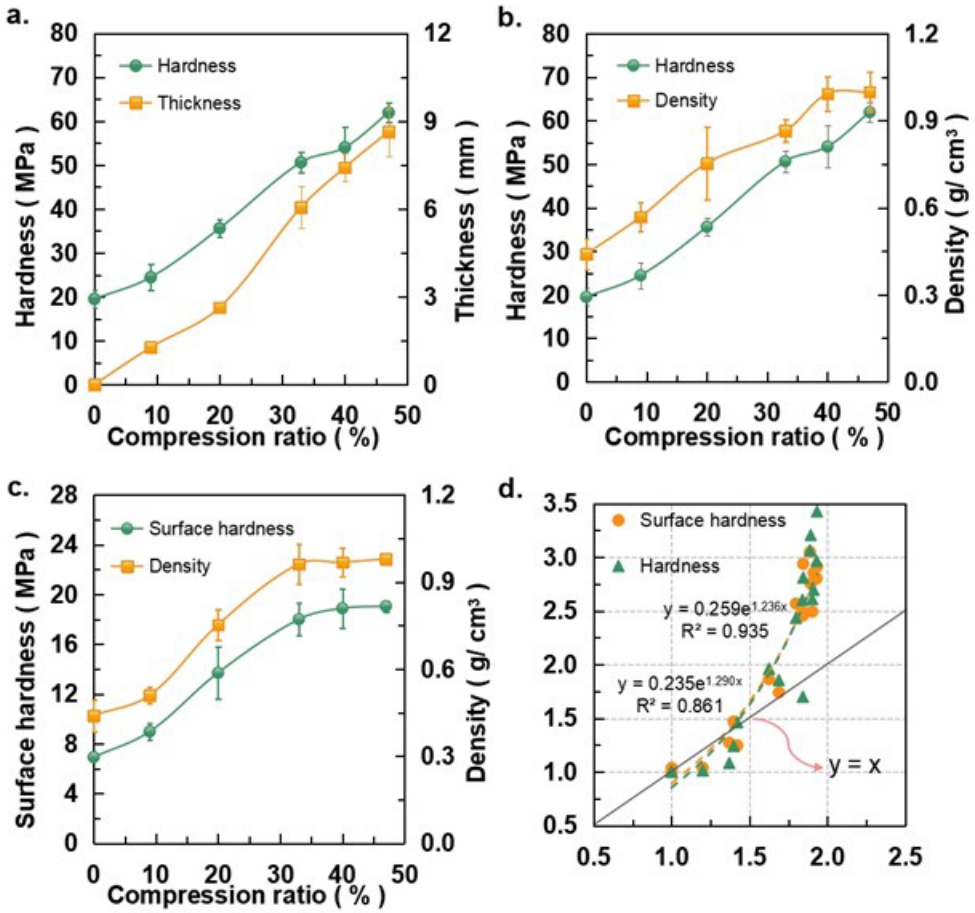

Fig. 11. Relationship between hardness, thickness, and density of the surface-compressed layer (a, b), and the relationship between surface hardness and density (c, d).

Comparison to Wood-Based Products

The results of this study indicated that surface-compressed wood had comparable mechanical properties to other structural materials, such as timber and raw wood. In addition, the surface-compressed wood showed anisotropic behavior, similar to that of sandwich fiber-reinforced composites. Further comparison of the bending properties of the traditional compressed wood and different wood-based commercial structures with the surface-compressed wood is shown in Fig. 12.

In this study, the surface density of the surface compressed wood significantly increased, resulting in a significant increase in MOE and MOR, and the advantage of the surface-compressed wood was its excellent specific stiffness and specific strength. The graph illustrated that the specific stiffness (27 to 30 × 106 m^2/s^2) of the surface-compressed wood was on the higher end of the natural composite (14 to 27 × 106 m^2/s^2) envelope. In addition, the specific strength (179 to 203 × 103 m^2/s^2) was slightly higher than other wood-based productions (65 to 197 × 103 m^2/s^2), and the selection and control of density and the compressed layer thickness could satisfy the actual needs of different wood products and structural materials. The failure mode of surface-compressed wood must also be considered in comparison to other materials.

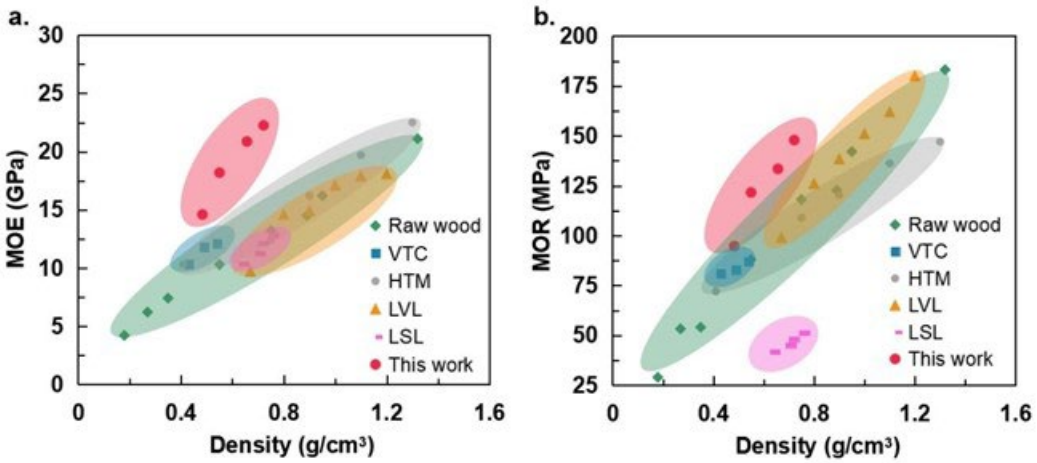

Fig. 12. Bending modulus *vs*. the bending strength for some traditional compressed wood (VTC denoted compressed woods by viscoelastic thermal compression (Kutnar *et al.* 2008), HTM denoted compressed woods using the thermo-hydro-mechanical method (Bao *et al*. 2017)) and construction materials (where LVL denoted laminated veneer lumber (Wei *et al.* 2019), LSL denoted laminated strand lumber (Denizli-Tankut *et al.* 2004)).

CONCLUSIONS

1. Surface-compressed wood was manufactured *via* surface soaking, preheating, and radial compressing at 180 °C. And this technology significantly improved physical and mechanical properties of fast-growing poplar wood, such as strength, stiffness, compression, and hardness.
2. Due to its sandwich density structure, the mechanical properties of the surface-compressed wood were different in the radial and tangential directions. The radial direction had slightly higher strength for all properties, except for full-surface transverse compressive strength. This increased capacity was attributed to the density gradient in the radial direction. The improved mechanical properties would also allow for the surface-compressed wood to be used in structural composites.
3. The surface-compressed wood formed a gradient distribution structure with a high surface density and low central density, while the surface layers of the materials had maximum tensile or compressive stresses in the bending performance test. Therefore, surface-compressed wood has greater modulus of rupture (MOR) and modulus of elasticity (MOE) than other wood products of the same density. The contribution of sandwich structure to MOR and MOE increase was positively correlated with wood surface density.
4. In addition, the results confirmed the assumption that low-density wood species could be successfully used for wood structural production if they were densified using a surface-compressed process.

ACKNOWLEDGMENTS

The authors acknowledge the financial support from the Special Scientific Research of the Forest Public Welfare Industry (Grant No. 31670557; 32071690). The authors thank LetPub (www.letpub.com) for linguistic assistance and pre-submission expert review.

REFERENCES CITED

Anshari, B., Guan, Z., Kiamori, A., Jung, K., and Komatsu, K. (2012). "Structural behaviour of glued laminated timber beams pre-stressed by compressed wood," *Construction and Building Materials* 29, 24-32. DOI: 10.1016/j.conbuildmat.2011.10.002

Bao, M. Z., Huang, X. A., Zhang, Y. H., Yu, W., and Yu, Y. (2016). "Effect of density on the hygroscopicity and surface characteristics of hybrid poplar compreg," *Journal of Wood Science* 62(5), 441-451. DOI: 10.1007/s10086-016-1573-4

Bao, M. Z., Huang, X. A., Jiang, M. L., Yu, W., and Yu, Y. (2017). "Effect of thermo-hydro-mechanical densification on microstructure and properties of poplar wood (*Populus tomentosa*)," *J. Wood Sci*. 63, 591-605. DOI: 10.1007/s10086-017-1661-0

Birman, V., and Kardomatea, G. A. (2018). "Review of current trends in research and applications of sandwich structures," *Composites Part B: Engineering* 142, 221-240. DOI: 10.1016/j.compositesb.2018.01.027

Cai, J. B., Yang, X., Cai, L. P., and Shi, S. Q. (2013). "Impact of the combination of densification and thermal modification on dimensional stability and hardness of poplar lumber," *Drying Technology* 31, 1107-1113. DOI: 10.1080/07373937.2013.775147

Cao, L. F., Chen, J. Y., Niu, Q. F., Shi X. W., and Li, T. Y. (2016). "Experimental study on local compression performance perpendicular to the grain for five different woods," *China Science Paper* 31(11), 1452-1456. DOI: 10.12677/ms.2021.112013

Denizli-Tankut, N., Smith, L. A., Smith, W. B., and Tankut, A. N. (2004). "Physical and mechanical properties of laminated strand lumber treated with fire retardant," *Forest Products Journal* 54(6), 63-70. DOI: 10.1520/d8223-19

Gao, Z. Q., Huang, R. F., Lu, J. X., Chen, Z. J., Guo, F., and Zhan, T. Y. (2016). "Sandwich compression of wood: Control of creating density gradient on lumber thickness and properties of compressed wood," *Wood Science Technology* 50(4), 833-844. DOI: 10.1007/s00226-016-0824-2

Gao, Z. Q., Huang, R. F., Chang, J. M., Li, R., and Wu, Y. M. (2019). "Effects of pressurized superheated-steam heat treatment on set recovery and mechanical properties of surface-compressed wood," *BioResources* 14(1), 1718-1730. DOI: 10.15376/biores.14.1.1718-1730

Garg, A., Belarbi, M., Chalak, H. D., and Chakrabarti, A. (2021). "A review of the analysis of sandwich FGM structures," *Composite Structures* 113427. DOI: 10.1016/j.compstruct.2020.113427

Gdoutos, E. E., Daniel, I. M., Wang, K. A., and Abot, J. L. (2001). "Nonlinear behavior of composite sandwich beams in three-point bending," *Experimental Mechanics* 41(2), 182-189. DOI: 10.1007/BF02323195

Huang, R. F., Wang, Y. W., Zhao, Y. K., and Lv, J. X. (2012). "Sandwich compression of wood by hygro-thermal control," *Mokuzai Gakkaishi* 58(2), 84-89. DOI:

10.2488/jwrs.58.84
Inoue, M., Norimoto, M., Otsuka, Y., and Yamada, T. (1990). "Surface compression of coniferous wood lumber I. A new technique to compress the surface layer," *Mokuzai Gakkaishi* 36(11), 969-975. DOI: 10.1515/hf.2000.112
Kawasaki, T., Zhang, M., Wang, Q., Komatsu, K., and Kawai, S. (2006). "Elastic moduli and stiffness optimization in four-point bending of wood-based sandwich panel for use as structural insulated walls and floors," *Journal of Wood Science* 52, 302-310. DOI: 10.1007/s10086-005-0766-z
Kitamori, A, Jung, K., Mori, T., and Komatsu, K. (2010). "Mechanical properties of compressed wood in accordance with the compression ratio," *Mokuzai Gakkaishi* 56(2), 67-78. DOI: 10.2488/jwrs.56.67
Kutnar, A., Kamke, F. A., Sernek, M. (2008). "The mechanical properties of densified VTC wood relevant for structural composites," *Holz Roh Werkst* 66, 439-446. DOI: 10.1007/s00107-008-0259-z
Kutnar, A., Kamke, F. A., Sernek, M. (2009). "Density profile and morphology of viscoelastic thermal compressed wood," *Wood Science Technology* 43(1-2), 57-68. DOI: 10.1007/s00226-008-0198-1
Laine, K., Segerholm, K., Wålinder, M., Rautkari, L., and Hughes, M. (2016). "Wood densification and thermal modification: Hardness, set-recovery and micromorphology," *Wood Science Technology* 50(5), 1-12. DOI: 10.1007/s00226-016-0835-z
Leijten, A. J. M., Larsen, H. J., Van der Put, T. A. C. M. (2010). "Structural design for compression strength perpendicular to the grain of timber beams," *Construction and Building Materials* 24, 252-257. DOI: 10.1016/j.conbuildmat.2009.08.042
Leijten, A. J. M. (2016). "The bearing strength capacity perpendicular to grain of Norway Spruce-Evaluation of three structural timber design models," *Construction and Building Materials* 105, 528-535. DOI: 10.1016/j.conbuildmat.2015.12.170
Li, J. (2014). *Wood Science*, Edition 3, Science Press, Beijing.
Li, R., Gao, Z. Q., Feng, S. H., Chang, J. M., Wu, Y. M., and Huang, R. F. (2018). "Effects of preheating temperatures on the formation of sandwich compression and density distribution in the compressed wood," *Journal of Wood Science* 64, 751-757. DOI: 10.1007/s10086-018-1758-0
Liu, Y. X., and Zhao, G. J. (2004). *Wood Resource Materials Science*. Beijing, China.
Marat-Mendes, R., Martins, R., and Reis, L. (2020). "Experimental and numerical characterization of stress-strain fields on sandwich beams subjected to 3PB and 4PB," *Composite Structures* 232, 111421. DOI: 10.1016/j.compstruct.2019.111421
Morsing, N. (2000). *Densification of Wood: The Influence of Hydrothermal Treatment on Compression of Beech Perpendicular to the Grain*, Ph.D. Dissertation, Technical University of Denmark.
Navi, P., and Pizzi, A. (2015). "Property changes in thermo-hydro-mechanical processing," *Holzforschung* 69(7), 863-873. DOI: 10.1515/hf-2014-0198
Sandberg, D., Haller, P., and Navi, P. (2013). "Thermo-hydro and thermo-hydro-mechanical wood processing: An opportunity for future environmentally friendly wood products," *Wood Material Science & Engineering* 8(1), 64-88. DOI: 10.1080/17480272.2012.751935
Seborg, R. M. (1945). "Heat stabilized compressed wood (staypak)," *Mech. Eng.* 67(1), 25-31. DOI: 10.1016/0016-0032(45)90235-3
Skyba, O., Niemz, P., and Schwarze, F. (2008). "Degradation of thermo-hygro-mechanically (THM)-densified wood by soft-rot fungi," *Holzforschung* 62(3), 277-

283. DOI: 10.1016/j.fbr.2007.09.001

Yan, L. (2010). *Mechanism and Application of Compressive Deformation Fixation of Poplar by Glycorin Pretreatment*, Ph.D. Dissertation. Beijing Forestry University, Beijing.

van der Put, T. A. C. M. (2008). "Derivation of the bearing strength perpendicular to the grain of locally loaded timber blocks," *Holz Roh Werks* 66, 409-417. DOI: 10.1007/s00107-008-0258-0

Wang, J. F., Wang, X., Zhan, T. Y., Zhang, Y. L., Lv, C., He, Q., Fang, L., and Lv, X. N. (2018). "Preparation of hydro-thermal surface-densified plywood inspired by the stiffness difference in sandwich structure of wood," *Construction and Building Materials* 177, 83-90. DOI: 10.1016/j.conbuildmat.2018.05.135

Wei, Y. N., Rao, F., Yu, Y. L., Huang, Y. X., and Yu, W. J. (2019). "Fabrication and performance evaluation of a novel laminated veneer lumber (LVL) made from hybrid poplar," *European Journal of Wood and Wood Products* 77, 381-391. DOI: 10.1007/s00107-019-01394-y

Zhan, J. F., and Avramidis, S. (2017). "Transversal mechanical properties of surface-densified and hydrothermally modified needle fir wood," *Wood Science Technology* 51(4), 721-738. DOI: 10.1007/s00226-017-0909-6

Zhong, W. Z., Rusinek, A., Jankowiak, T., Abedd, F., Bernierb, R., and Suttereand, G. (2015). "Influence of interfacial friction and specimen configuration in Split Hopkinson pressure bar system," *Tribology International* 90, 1-14. DOI: 10.1016/j.triboint.2015.04.002

Zhong, W. Z., Deng, Z. F., Huang, X. C., and Hao, Z. M. (2016). "Anisotropic mechanical behavior of spruce under medium strain rate loading," *Chinese Journal of Theoretical and Applied Mechanics* 33(5), 25-33. DOI: 10.7498/aps.51.2320

Article submitted: February 2, 2022; Peer review completed: May 14, 2022; Revised version received and accepted: May 18, 2022; Published: May 24, 2022.
DOI: 10.15376/biores.17.3.4280-4296